

Thermodynamic model of a single stage H₂O-LiBr absorption cooling

Siham Ghatos^{1,*}, *Mourad Taha Janan*¹, and *Abdessamad Mehdari*¹

¹Laboratory of Applied Mechanics and Technologies (LAMAT), ENSET, STIS Research Center; Mohammed V University in Rabat, Morocco.

Abstract. Due to the dangerous ecological issues and the cost of the traditional energy, the use of sustainable power source increased, particularly solar energy. Solar refrigeration and air conditioner such as, absorption solar systems denote a very good option for cooling production. In present work, an absorption machine that restores the thermal energy produced by a flat plate solar collector in order to generate the cooling effect was studied. For the seek of good performances, it is necessary to master the modeling of the absorption group by establishing the first and second laws of the thermodynamic cycle in various specific points of the cycle. The main objective was to be able to finally size different components of the absorption machine and surge the coefficient of performance at available and high heat source temperature. A model were developed using a solver based on Matlab/Simulink program. The obtained results were compared to the literature and showed good performances of the adopted approach.

1 Introduction

This nowadays, air conditioning is generally provided by classic mechanical compression machines that consume a considerable amount of electrical energy in addition to the toxic fluids used inside. An alternative is to use the solar-powered refrigeration cycles instead. Among the possible solutions, absorption cycles are the most technologically mature and use natural refrigerants such as water. In addition, this technology only requires thermal solar panels because of the low temperature required. Mechanical compression machines often have a higher coefficient of performance (COP) compared to the solar absorption systems, this issue is overcome by the long-term efficiency and the pollution elimination.

The literature reveals several studies that have been conducted on absorption refrigeration systems. Gutiérrez-Urueta et al. [1] treated conventional absorption models of H₂O/LiBr. The characteristic equations used in this study were developed by Hellmann et al. (1998) and represent an experimental evaluation of chiller performance. Karamangil et al. [2] have presented a thermodynamic analysis of single-stage absorption applying various refrigerant-absorbent pairs. The comparison between different theoretical system performances have proved that the coefficient of performance values decreases as the absorber and condenser temperatures decrease, and increase as the evaporator and condenser temperatures increase. A trial work of solar cooling absorption cycles executed in Reunion Island was devoted by Marc et al. [3], the objective is to attain an effective cooling of classrooms using a solar-powered cooling machine without any

reinforcement techniques (cold or hot). The work of Gomri et al. [4] has shown that when the condenser-absorber and the evaporator temperatures are changed from 33°C to 39°C, 4°C to 10°C, respectively, the COP values of the single, double and triple effect absorption system are arranged between 0.73–0.79, 1.22–1.42, 1.62–1.90, respectively. The exergetic efficiency values for single, double and triple effect absorption cycle are in the range of 17.7–25.2%, 14.3–25.1%, 12.5–23.2%, respectively. Dynamic simulation of an absorption refrigeration endo-reversible system is established to minimize the time optimization and reach a maximum value of the chiller efficiency using a method that combines heat and mass transfer principles [5]. A dynamic model of a single-effect Absorption Refrigeration System (ARS) using LiBr–H₂O as work fluid, to evaluated the influence of thermal masses of each component, the method is solved by the fourth-order Runge–Kutta and the results showed that the thermal load of condenser and generator are reliant on the condenser thermal mass. However, the thermal load of the absorber and evaporator are hardly influenced by thermal masses [6]. Assilzadeha et al. [7] presented a comparison between conventional mechanical compression and solar absorption air conditioning systems, they showed that this latter has more advantages. Balghouthi et al. [8] have shown that the high use of conventional air conditioning technologies has led to increasing environmental problems in addition to the cost of fossil fuels while the solar resource is free. As for any thermal system, it is necessary to study the evolution of the process and determine the main intervening factors that contribute to its performance. Ketfi et al. [10] have described the

* Corresponding author: ghatossiham@gmail.com

thermal behavior of different elements of a single-stage solar absorption machine functioning with LiBr-H₂O (YAZAKI WCFSC5) with 17.6 kW cool operating in Algerian climate. Ghatos et al. [11] is preferred to work with a generator temperature where the coefficient of performance reaches its maximum value.

The present work aims to establish and solve a detailed model of a single effect absorption refrigeration system working with H₂O-LiBr binary pair. A simulation program has been realized to describe the thermodynamic analysis of different components in a typical single stage solar absorption machine. The thermal and physical properties of the binary mixture are calculated in each stage of the absorption cycle in order to determine the coefficient of performance, and therefore, improve the working conditions of the system.

2 Thermodynamic model

2.1 System description

As shown in figure 1, the ARS contains a condenser (c), expansion valve (V₁), evaporator (e), absorber (a), pump (p), reducing valve (V₂), a solution heat exchanger (SHE) and generator (g). The terms Q_g, Q_c, Q_a and Q_e denote the heat transfer rate from the generator, condenser, absorber, and evaporator, respectively. In the machine operation, the water vapor leaving the evaporator is mechanically absorbed by the strong bromide lithium solution (high concentration) in the absorber. The weak solution (low concentration) is pumped from the absorber to the generator in which the H₂O/LiBr refrigerant-absorber pair is separated, the superheated refrigerant (water vapor) leaves the generator to the condenser and the strong solution goes down to the absorber by a reducing valve. In the condenser, the generated steam is condensed and the water at the high pressure passes via an expansion valve to evaporate in the lower pressure in the evaporator where the whole process starts again. The heat exchanger between the absorber and generator is regularly applied to increase the COP by preheating the weak solution going up to the generator.

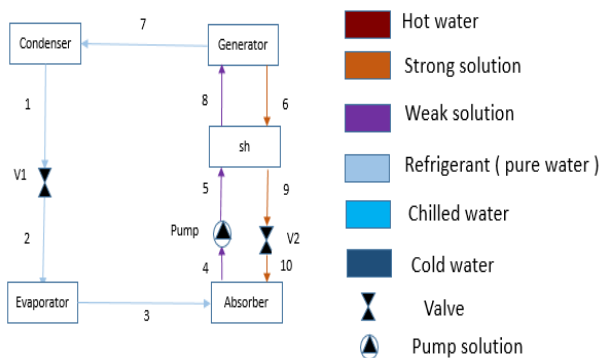


Fig. 1. Single effect absorption cooling cycle.

The heat exchanger modeling is taken into consideration using the pair (H₂O/LiBr) as the operating fluid under the following considerations [12]:

- The evolutions in the four primary exchangers (generator, condenser, evaporator and absorber) was assumed adiabatic.
- The refrigerant came out of the condenser were considered as saturated liquid at the corresponding temperature and pressure.
- The heat exchanged with the surroundings and pressure drops were neglected.
- The refrigerant at the outlet of the evaporator was a saturated steam at the temperature and pressure of evaporation.

2.1 Formulation of analysis model

The mass and energy balance equations for each heat exchanger can be expressed as follows:

$$\begin{aligned} \dot{m}_w &= \dot{m}_6 = \dot{m}_7 + \dot{m}_8 \\ X_w &= X_6 \\ X_s &= X_8 \\ \dot{m}_6 X_6 &= \dot{m}_7 + \dot{m}_8 X_8 \\ Q_g &= m_7 h_7 + m_8 h_8 - m_6 h_6 \end{aligned} \quad (1)$$

Q_g being the thermal power activation and m the mass flow rates.

With X_s and X_w representing the concentrations of the strong and weak LiBr solution, respectively. h the enthalpy of the solution at different levels of the generator.

$$\begin{aligned} \dot{m}_r &= \dot{m}_7 = \dot{m}_1 \\ Q_c &= m_1 (h_1 - h_7) \end{aligned} \quad (2)$$

Q_c being the heat flux of the condenser With m_r the refrigerant mass flow rate.

$$\begin{aligned} \dot{m}_r &= \dot{m}_3 = \dot{m}_2 = \dot{m}_1 = \dot{m}_7 \\ Q_e &= m_1 (h_3 - h_2) \end{aligned} \quad (3)$$

Q_e being the cooling capacity.

$$\begin{aligned} \dot{m}_r + \dot{m}_s - \dot{m}_w &= 0 \\ \dot{m}_s X_s - \dot{m}_w X_w &= 0 \\ Q_a &= \dot{m}_4 h_4 - \dot{m}_3 h_3 - \dot{m}_{10} h_{10} \end{aligned} \quad (4)$$

Q_a being the heat flux of the ab.

$$\begin{aligned} T_9 &= T_5 E + T_8 (1 - E) \\ h_6 &= h_5 + \frac{\dot{m}_8}{\dot{m}_5} (h_8 - h_9) \end{aligned} \quad (5)$$

With E the thermal efficiency of the solution heat exchanger.

The specific solution flow rate f is defined as the ratio of the weak solution mass flow rate (\dot{m}_w) on the

refrigerant masse flow rate (\dot{m}_r) generated in the generator [14]:

$$f = \frac{\dot{m}_w}{\dot{m}_r} = \frac{X_s}{X_s - X_w} \quad (6)$$

The strong and weak solutions concentrations are given by Lansing [13] as:

$$X_d = \frac{49,04 + 1,125.T_{ab} - T_c}{134,65 + 0,47.T_{ab}} \quad (7)$$

$$X_c = \frac{49,04 + 1,125.T_g - T_c}{134,65 + 0,47.T_g} \quad (8)$$

X_s : The strong solution concentration.
 X_w : The weak solution concentration.

The coefficient of performance (COP) defined by the ratio of the amount of heat absorbed by the evaporator on the amount of heat supplied to the generator (plus the pumps work if not neglected):

$$COP = \frac{Q_e}{Q_g + W_p} \quad (9)$$

Q_e : Amount of heat absorbed by the evaporator.
 Q_g : Amount of heat absorbed by the generator.
 W_p : Work of the solution pump.

The coefficient of performance (COP) can be expressed using the previous expressions of heat quantities and work:

$$COP = \frac{h_3 - h_2}{h_7 + (f - 1)h_8 - f(h_6 + h_4 - h_5)} \quad (10)$$

The efficiency of the system is defined as the actual coefficient of performance (COP) divided by the ideal coefficient of performance (COP_c).

$$\eta = \frac{1}{\left(\frac{T_g - T_{ab}}{T_g}\right)\left(\frac{T_e}{T_c - T_e}\right)} \times \frac{h_3 - h_2}{h_7 + (f - 1)h_8 - f(h_6 + h_4 - h_5)} \quad (11)$$

The equilibrium pressure of water (refrigerant) as a function of temperature is given by the following empirical equations [15]:

$$P = P_{exp} \left(\frac{T_c}{T_k} \sum \alpha \right) \quad (12)$$

$$\sum \alpha = U_0 T_0 + U_1 T_0^{1.5} + U_2 T_0^3 + U_3 T_0^{3.5} + U_4 T_0^4 + U_5 T_0^{7.5}$$

The coefficients U_i are given in table 1 below:

Table 1. Coefficients for the calculation of α

i	U
0	-7,85823
1	1,8399
2	-11,781
3	22,6705
4	-15,9393
5	1,77516

The specific heat of the LiBr solution with concentration X is given by [14]:

$$Cp(X) = (2,01.X_0^2 - 5,15.X_0 + 4,23) \quad (13)$$

$$X_0 = \frac{X}{100}$$

The enthalpy of liquid water with temperature T, in the case of the condenser outlet, is given by [14]:

$$h_{liq}(T) = 4.185T \quad (14)$$

The enthalpy of the water vapor, in the case of the evaporator, is given by the following empirical equation [14]:

$$h_v(T) = -125397.10^{-8}T^2 + 1,88060937T + 2500,559 \quad (15)$$

The enthalpy of the H₂O/LiBr solution mixture at the level of the generator and the absorber are given by:

◆ **For 0% < X < 40% LiBr**

$$h = \left[\begin{array}{l} U_0 + U_1.X + U_2.X^2 \\ + WT.(V_0 + V_1.X + V_2.X^2) \end{array} \right] .3,326 \quad (16)$$

$$WT = \frac{9}{5}.T + 32$$

The coefficients U_i and V_i are given in Tab. 2.

Table 2. The coefficient (U, V) for the calculation of h (T, X)

i	U	V
0	-33,1054264	1,0090734
1	0,13000636	-0,01377507
2	0,00097096	0,000085131

◆ **For 45% < X < 70% LiBr**

$$\begin{aligned}
 h &= \sum U + T \sum V + T^2 \sum W \\
 \sum U &= U_0 X^0 + U_1 X^1 + U_2 X^2 + U_3 X \\
 \sum V &= V_0 X^0 + V_1 X^1 + V_2 X^2 + V_3 X \\
 \sum W &= W_0 X^0 + W_1 X^1 + W_2 X^2 + W_3 X \quad (17)
 \end{aligned}$$

Table 3. The coefficients involved in the expression above are given in

i	U	V	W
0	-2024,33	18,2829	-0,037008214
1	163,309	-1,1691757	0,0028877666
2	-4,88161	0,03248041	-0,000081313015
3	0,06302948	-0,0004034184	-0,00000099116628
4	-0,0002913704	0,0000018520569	- 0,000000004444120

The simulation flowchart for the thermodynamic properties of the absorption cycle was represented in algorithm (See F).

The solution density of the LiBr was given by [16]:

$$\begin{aligned}
 dLiBr &= 1145,36 + 470,84 X_0 + 1374,79 X_0^2 \\
 &\quad - (0,333393 + 0,571749 X_0)(T + 273,15) \quad (18)
 \end{aligned}$$

3 Results and discussion

A simulation, using the developed tool has been carried out to study the influence of the working temperatures on the heat transfer rates and the coefficient of performance. The following data were adopted for this simulation.

Table 4. Thermodynamic properties of LiBr-H₂O in the cycle

Point i	T _i (°C)	P _i (kPa)	X _i (%LiBr)	h _i (kJ/kg)	m _i (kg.s ⁻¹)
1	32,0	4,7576	0	133,92	0,0006
2	5,0	0,8725	0	133,92	0,0006
3	5,0	0,8725	0	2509,93	0,0006
4	28,0	0,8725	51,1061	57,7252	0,0044
5	28,0	4,7576	51,1061	57,7276	0,0044
6	56,0	4,7576	51,1061	112,32	0,0044
7	75,0	4,7576	0	2657,30	0,0006
8	75,0	4,7576	59,6910	181,91	0,0038
9	42,1000	4,7576	59,6910	118,14	0,0038
10	42,1000	0,8725	59,6910	118,14	0,0038

For the parametric study of the absorption system, the choice was made to work with a generator temperature of 80 to 100°C and a condenser temperature of 34, 35 & 39 °C with an evaporator temperature fixed at 5°C & 35 °C . The efficiency of the solution heat exchanger was considered to be 0.7.

The parametric study allowed to present the variation of the coefficient of performance with the generator temperature as depicted in Fig. 3. We noticed that when increasing the condenser temperature (T_c) the COP decreases, this is explained by the high condensation temperature that causes problems in the condensation process. It can be noticed that an increase in the generator temperature (T_g) increases the COP until arriving in the stabilization temperature above 90°C, going above certain generator temperature will cause some problems in the binary mixture entering the absorber, namely the crystallization effect and therefore improper operation of the machine.

In Fig. 4, the coefficient of performance (COP) decrease with increasing the condenser temperature (T_c), this decreasing were significant if the generator temperature was low. Thus, at higher generator temperatures (T_g) (above 90°C), the COP starts to balance out. For the condenser, the water vapor should be cooled for better condensation, the cooling can be possible by utilizing cooling towers or natural air cooling.

The increase in evaporation temperature (T_e) increases the (COP) as seen in Fig. 5, the temperature of the evaporator sets the low pressure. Thus, the higher the generator temperatures (T_g), the lower the variation in COP, which confirms the results previously found (Fig. 4).

To control the variation of COP, we set the variation of absorber temperature between 20°C and 39°C. The efficiency of the system was fixed at 0.7 and the evaporator temperature was chosen to be 5°C. The generator temperatures has been set respectively to 80°C, 90°C and 100°C. The condensation temperature T_c was taken equal to 35°C. The parametric study allows showing the temperature of the absorber (T_a) leads to a decrease in the COP (Fig. 6). On the other hand, at the generator, the temperatures relatively high (over 90°C), the COP tends to stabilize.

According to the Fig.7, it can be seen that increasing the efficiency of the solution exchanger (E) increases the coefficient of performance (COP), which explains, why it was part of all absorption machines.

In order to obtain the COP value to be high, it was preferable to work with higher generator temperatures.

At Increased temperature of the evaporator, the generator caused a slightly increase of heat in the condenser. So, at the more T_g and T_c higher the quantity Q_g and Q_a was low because the increase of T_g and T_e lowers the coefficient of performance specifically the heat produced at the generator Q_g. As well as, the variation in evaporator temperature does not influenced the amount of heat of the evaporator; it depended only on the given cooling capacity (Fig. 7 and Fig. 8).

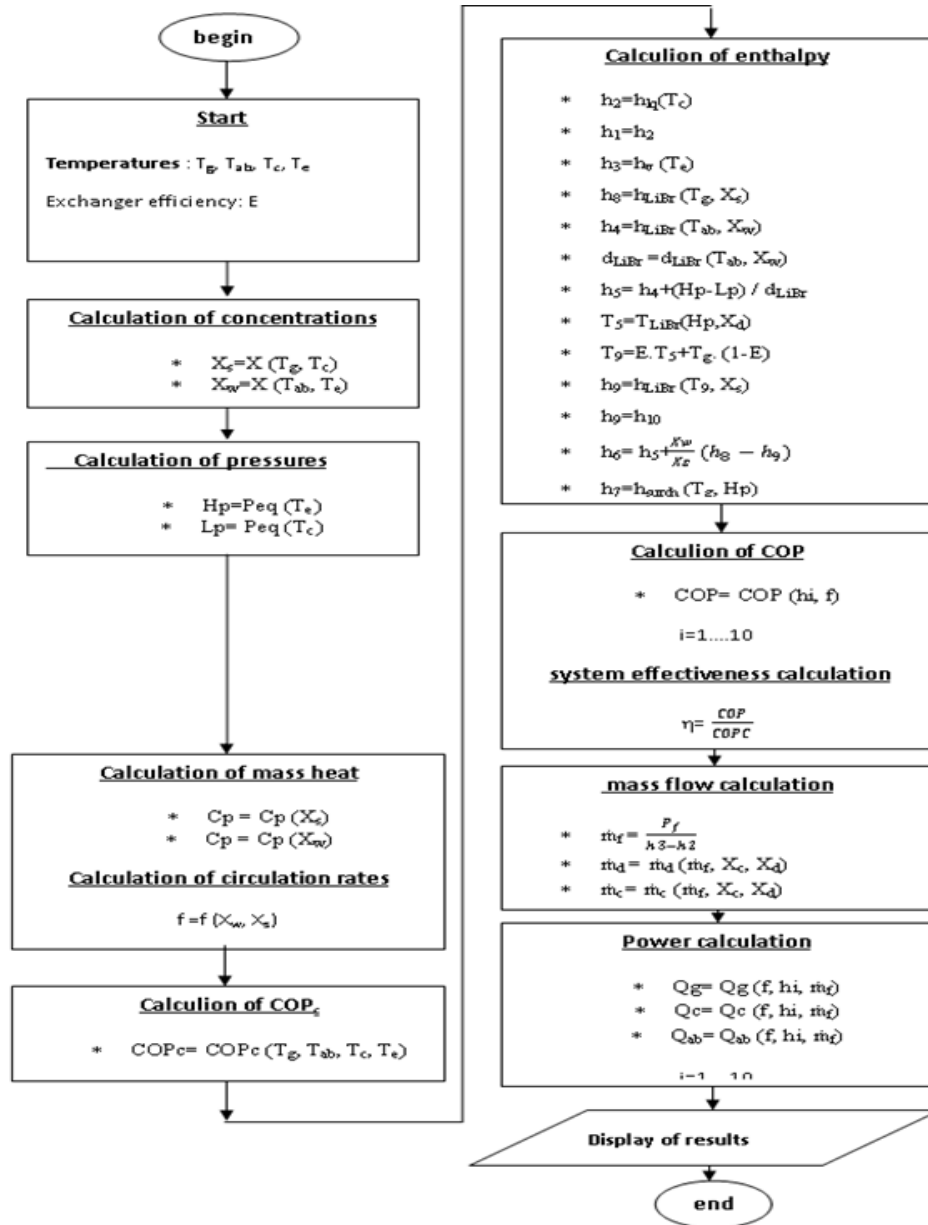


Fig. 2. Simulation flowchart for the single effect absorption chiller

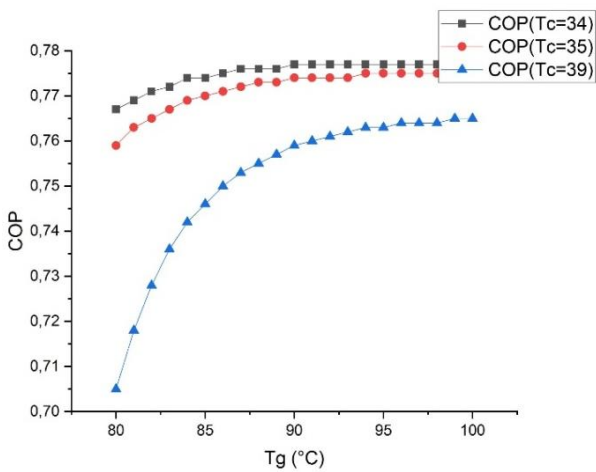


Fig. 3. The variation of COP with the generator temperature.

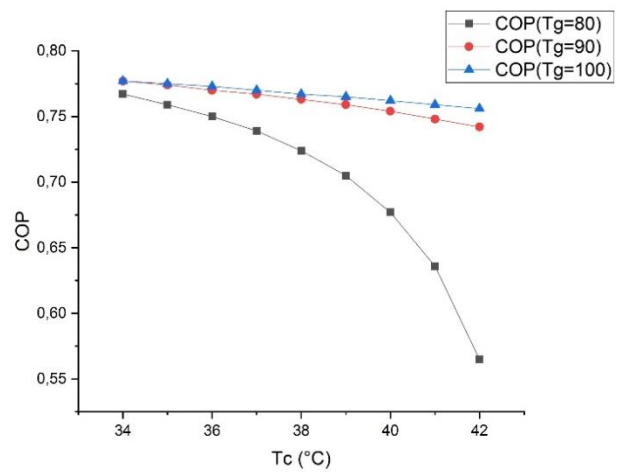


Fig. 4. The variation of COP with the condenser temperature.

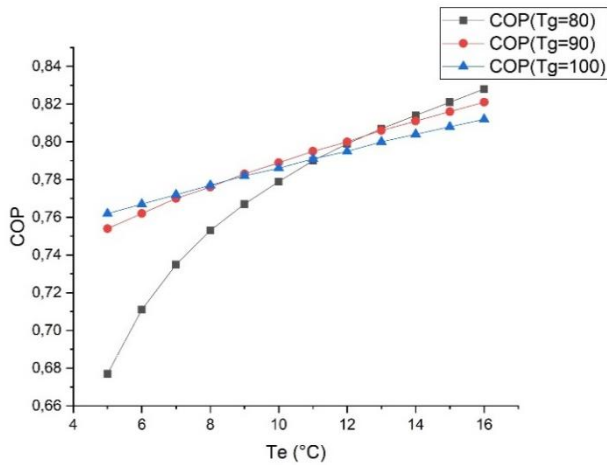


Fig. 5. The variation of COP with the evaporator temperature

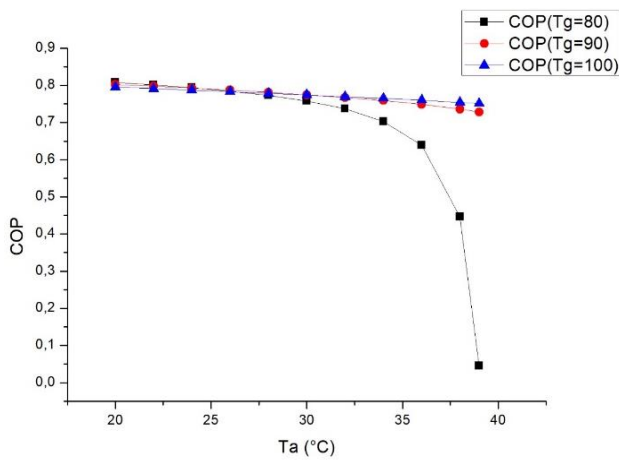


Fig. 6. The variation of COP with the evaporator temperature

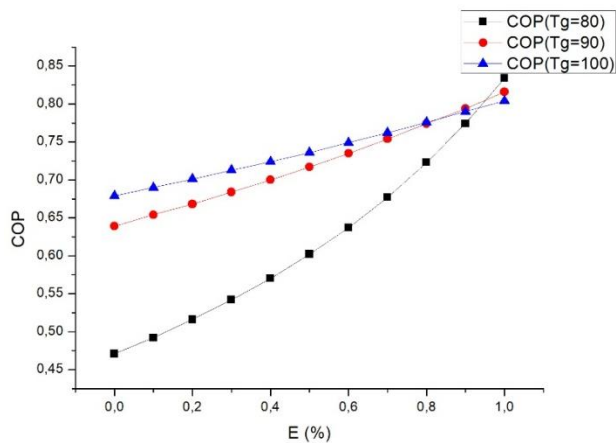


Fig. 7. Effect of heat exchanger efficiency (E) on the COP

With increasing the temperature of the evaporator and generator cause a slight increase the heat in the condenser. So, more the T_g and T_e higher the quantity of Q_g and in contrast, Q_a was observed low because the increase of T_g and T_e lower the coefficient of performance, specifically the heat produced at the generator Q_g . Further, the variation in evaporator temperature does not influence the amount of heat of the evaporator; it depending only on the given cooling capacity (figure 8 and 9).

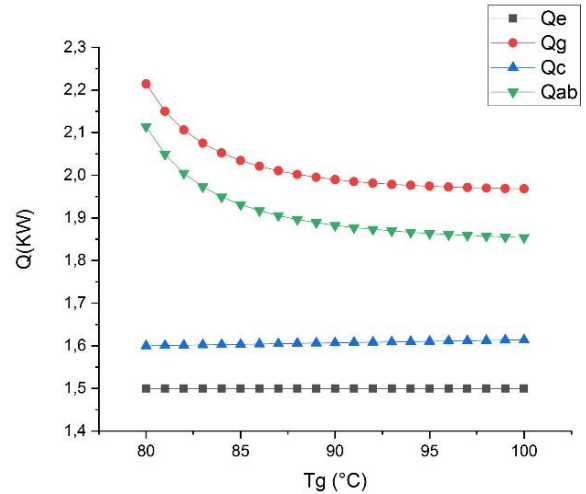


Fig. 8. The variation of heat transfer rate with the generator temperature.

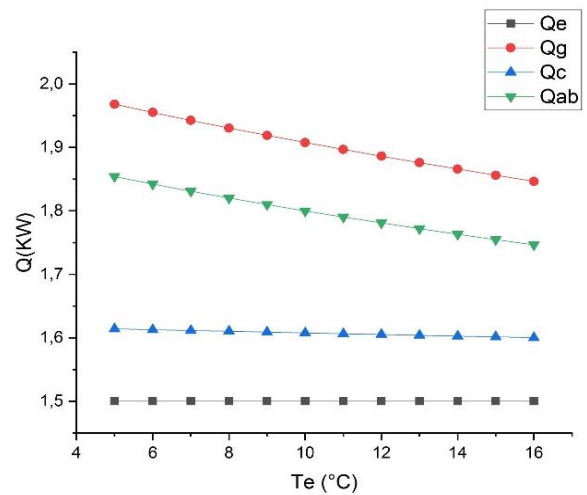


Fig. 9. The variation of heat transfer rate with the evaporator temperature.

4 Conclusion

In this paper, the first and second law of thermodynamics were used to model a single effect absorption refrigeration cycle. The impact of various temperatures, such as namely at the generator, the evaporator, the absorber, and the condenser, on the heat transfer rate for every element Q_a , Q_b , Q_c , Q_g was studied. At different temperatures at various regions the coefficient of performance COP was calculated. The examined system from the thermodynamic properties allowed to calculate the maximum values of the COP and thermal loads by varying the temperatures of different components using a developed mathematical model under MATLAB simulation program. When the evaporator temperature was varied from 5°C to 16°C , the coefficient of performance values of the single effect refrigeration system are in the range of 0,677 to 0,828. The absorber temperature in the range of 20°C to 39°C the COP was estimated 0,046 to 0,8. We have obtained the maximum value of COP at generator temperature between 80°C and 100°C was 0,777.

Nomenclature

COP: coefficient of performance
HP: high pressure
LP: low pressure
m: mass flow rate (kg/s)
P: pressure (Pa)
Q: heat transfer rate (kW)
T: temperature (°C)
W: mechanical power (kW)
X : concentration of solution at the exit of generator and absorber
d: density (kg/m³)
h: enthalpy (kJ)
c_p : mass heat of the LiBr solution at constant pressure (kJ kg⁻¹. K⁻¹)
T: temperature (°C)
Q: heat transfer rate (kW)
E : exchanger efficiency
f: flow rate

Greek symbols

η : efficiency

Superscripts and subscripts

c : condenser
e : evaporator
g : generator
a : absorber
s : strong
w : weak
V₁ : refrigerant expansion valve
V₂ : solution expansion valve
i : input
p : pump
f : liquid phase
v : vapor phase
liq : liquide phase
SHE : Heat exchanger
ABS : Asorption Refrigeration System

References

1. Gutiérrez-Urueta G, Rodríguez P, Ziegler F, Lecuona A, Rodríguez-Hidalgo MC. Extension of the characteristic equation to absorption chillers with adiabatic absorbers. *Int J Refrig* 2012;35:709–18.
2. Karamangil MI, Coskun S, Kaynakli O, Yamankaradeniz N. A simulation study of performance evaluation of single-stage absorption refrigeration system using conventional working fluids and alternatives. *Renewable and Sustainable Energy Reviews* 2010;14:1969–78.
3. Marc O, Lucas F, Sinama F, Monceyron E. Review experimental investigation of a solar cooling absorption system operating without any backup system under tropical climate. *Energy and Buildings* 2010;42:774–82.
4. Gomri R. Investigation of the potential of application of single effect and multiple effect absorption cooling systems. *Energy Convers Manage* 2010;51(8):1629–36.
5. Hamed M, Fellah A, Ben Brahim A. Optimization of a solar driven absorption refrigerator in the transient regime. *Applied Energy* 2012; 92:714–24.
6. A. Iranmanesh et M. A. Mehrabian, « Dynamic simulation of a single-effect LiBr–H₂O absorption refrigeration cycle considering the effects of thermal masses », *Energy Build.*, vol. 60, p. 47-59, mai 2013.
7. R. Touaibi, E. E. Vasilescu, M. Feidt, A. Kheiri, M. T. Abbes, et B. Khelidj, « à simple effet utilisant le couple Eau – Bromure de lithium », p. 6.
8. M. Balghouthi, M.H. Chahbani, A. Guizani “Feasibility of solar absorption air conditioning in Tunisia” *Building and environment* 43, pp.1459-1470, 2008.
9. Ketfi, O., Merzouk, M., Merzouk, N. K., & El Metennani, S. (2015, December). Modeling and simulation of a single stage solar absorption cooling machine under Algerian climate. In 2015 3rd International Renewable and Sustainable Energy Conference (IRSEC) (pp. 1-5). IEEE.
10. Yazaki, Absorption cooling machine WFC-SC20, YAZAKI Europe Limited 2007.
11. Ghatos S , Taha-Janan M, Mehdari A (2019, novembre). Modelling and Simulation of a Single Effect Solar Absorption Cooling System H₂O-LiBr. . In 2019 7th International Renewable and Sustainable Energy Conference (IRSEC) IEEE.
12. S. Aprhornratana et I. W. Eames, « Thermodynamic analysis of absorption refrigeration cycles using the second law of thermodynamics method », *Int. J. Refrig.*, vol. 18, no 4, p. 244-252, mai 1995.
13. Muhsin Kilic, Omer Kaynakli.Theoretical Second law-based thermodynamic analysis of water-lithium bromide absorption refrigeration system. July 2004
14. Lansing, F. L. "Computer modeling of a single stage lithium bromide/water absorption refrigeration unit." *Jet Propulsion Laboratory, California Institute of Technology, Pasadena, CA, Deep Space Network Progress Report 42 (1976): 247-257.*
15. J. Patek, J. Klomfar. A computationally effective formulation of the thermodynamic properties of LiBr–H₂O solutions from 273 to 500 K over full composition range. *International Journal of Refrigeration* 29;566–578, (2006).
16. Lee RJ, DiGuilio RM, Jeter SM, Teja AS. Properties of lithium bromide–water solutions at high temperatures and concentration. II. Density and viscosity. *ASHRAE Trans.* 96(Pt. 1):709–28, (1990).